

Experimental characterization of domain walls dynamics in a photorefractive oscillator

Adolfo Esteban-Martín¹, Victor B. Taranenko^{1,2}, Javier García¹, Eugenio Roldán¹, and Germán J. de Valcárcel¹

¹*Departament d'Òptica, Universitat de València,
Dr. Moliner 50, 46100-Burjassot, Spain and*

²*Institute of Physics, National Academy of Sciences of the Ukraine, Kiev, Ukraine*

Abstract

We report the experimental characterization of domain walls dynamics in a photorefractive resonator in a degenerate four wave mixing configuration. We show how the non flat profile of the emitted field affects the velocity of domain walls as well as the variations of intensity and phase gradient during their motion. We find a clear correlation between these two last quantities that allows the experimental determination of the chirality that governs the domain walls dynamics.

PACS numbers: 42.65.Sf, 47.54.+r, 42.65.Hw

INTRODUCTION

Extended nonlinear systems with broken phase invariance (e.g., systems with only two possible phase values for a given state), are common in nature. These systems may exhibit different types of patterns but, importantly, the broken phase invariance lies at the origin of the appearance, in particular, of domain walls (DWs) which are the interfaces that appear at the boundaries between two spatial regions occupied by two different phase states [1, 2, 3].

In nonlinear optics there are several examples of spatially extended bistable systems that can show solutions for the emitted field with a given amplitude but opposite phases (that is, phases differing by π), such as degenerate optical parametric oscillators (DOPOs) or intracavity degenerate four-wave mixing [4]. The interface which connects both solutions, the DW, can be of either one of two different types: On the one hand, there are Ising walls in which the light intensity of the field at the core of the interface is zero and the phase changes abruptly from ϕ to $\phi + \pi$; on the other hand, there are Bloch walls in which the light intensity never reaches zero and the change of phase is smooth across the DW [5]. In addition to this, Ising walls are always static whereas Bloch walls are usually moving fronts (they are static only when the system is variational what is an uncommon situation for dissipative systems). It is important to remark that Bloch walls are chiral (they are not identical to their mirror images) as in the Bloch wall the phase angle rotates continuously through π and two directions of rotation are possible. This fact has important dynamical consequences as Bloch walls with opposite chirality move in opposite directions [5]. Both Ising and Bloch walls have been found in nonlinear optical cavity experiments [6, 7].

When a control parameter is varied a bifurcation that changes the nature of the DW may happen. This is the nonequilibrium Ising-Bloch transition (NIBT) that has been investigated theoretically in [5, 8] and has been repeatedly observed in liquid crystals (see, e.g., [9, 10]). In the context of nonlinear optical systems, the NIBT has

been predicted to occur in type I [11] and type II [12] DOPOs, in intracavity type II second-harmonic generation [13], and in vectorial Kerr cavities [14]. Recently, we have reported the first observation of this phenomenon, the NIBT, in an optical system, namely a photorefractive oscillator [7]. Moreover, our observation is rare in the sense that we observed a hysteretic NIBT [7, 15].

The aim of the present work is to study in detail the dynamics of the DWs we reported in [7] by means of the measurement of the different DWs characteristics, namely intensity, phase gradient and velocity, establishing relations among them. In particular, we consider whether the chirality parameter, which will be described later on, is appropriate for characterizing the DW.

EXPERIMENTAL SETUP

Our experimental setup, Fig.1, is a single-longitudinal mode photorefractive oscillator (PRO) formed by a Fabry Perot resonator in a near self-imaging arrangement [16] chosen in order to achieve a high Fresnel number [17, 18]. The nonlinear material, a BaTiO₃ crystal, is pumped by two counterpropagating laser beams of the same frequency. In this way a degenerate four wave mixing process occurs within the cavity. The degeneracy implies that the field exiting the nonlinear cavity is phase-locked and only two values of the phase (differing by π) are allowed [19]. Hence DW formation is allowed.

The system performance is ruled by different parameters such as detuning (which is the difference between the frequency of the pump and the frequency of the cavity longitudinal mode in which emission occurs), gain, losses and diffraction. All these parameters can be controlled up to some extent. We choose as in [7, 18] cavity detuning as the control parameter as it can be finely tuned in an actively stabilized system [20].

Regarding diffraction, the system is intentionally made quasi-one dimensional in the transverse dimension (1D system) in order to avoid the influence of DW curvature in the observed dynamics: Curvature induces a move-

ment in the DW [4, 12] that contaminates that due to the nature of the DW (i.e., its Ising or Bloch character). This is achieved by properly placing slits inside the nonlinear cavity (D in Fig. 1), in particular, at the Fourier planes (FP in Fig. 1). The width of the slits is adjusted to the size of the diffraction spot in these planes. In this way beams with too large inclination (such that their transverse wavevector falls outside the plane defined by the center line of the slit) are not compatible with the diffraction constraints of the cavity. This Fourier filtering allows the use of finite width slits and still gets rid of most 2D effects. It is also by using a diaphragm that spatial frequencies belonging to other longitudinal modes than the one of interest are removed [18].

Detuning, our control parameter, can be changed by means of a piezo-mirror. Depending on detuning, different types of structures can be found [17, 18, 21, 22] but for our present purposes it suffices to say that DWs exist in resonance or for positive cavity detuning (i.e., when the frequency of the pumping field is smaller than the frequency of the nearest cavity mode): At zero (or small positive) cavity detuning DWs are static (Ising type), whilst they start moving (Bloch type) if detuning is increased enough [7].

INJECTION OF DOMAIN WALLS

DWs can form spontaneously from noise when the detuning value lies in the appropriate domain, as it was the case with the DWs reported in [17, 18]. But waiting for the appearance of DWs from noise is not the most adequate strategy for their study for several reasons. On the one hand one must wait until the formation of the DW occurs and it is very likely that not a single DW but some of them appear, which complicates the analysis because of DW interaction. On the other hand even when a single structure is formed from noise, there is the problem that its position on the transverse plane will not always be the same. Owing to these and other reasons it is most convenient to find a way for injecting, or writing, DWs at will.

An injection technique to remove the initial structure and write a single DW has been devised [7, 23]. It consists in injecting, for a short time (the shutter in Fig. 1 remains open for a few seconds), a laser beam into the photorefractive oscillator that is tilted with respect to the resonator axis. This tilted beam has a phase profile in the transverse dimension x given by $\phi(x) = \phi_0 + (2\pi/\lambda \sin \alpha)x$, being ϕ_0 a constant, λ the light wavelength, and α the tilt angle with respect to the resonator axis.

Now, this injected tilted beam forces a phase variation, along the transverse dimension, of the intracavity field phase, but given the phase sensitive nature of the degenerate four-wave mixing process [19], only two

phase values (say 0 and π , modulo 2π) can be amplified. Thus, the regions of the field whose phase lies in the domain $]-\pi/2, +\pi/2[$ will be attracted towards the 0 phase value, whilst those with a phase lying in the domain $]\pi/2, +3\pi/2[$ will be attracted towards the phase value π .

As an immediate consequence, the appearance of a DW is forced as the points at which $\phi = \pm\pi/2$ (modulo 2π). These DWs are dark because those phase values cannot be amplified but also, and this is a more fundamental reason, because these points separate adjacent domains with opposite phases. These points, the DWs, are thus topological defects [26] what makes them very robust as they cannot be removed via continuous changes.

In Fig. 2 we show several snapshots of the interferogram of the output field during the writing process. In Fig. 2a the initial homogeneous field is shown, and the interferogram shows the homogeneity of the field phase. Then, in Fig. 2b the tilted beam is injected. While the injection is being applied, a blurred DW appears on the left, Fig. 2c, and moves to the right, Figs. 2d-2e. When the wall is located at the centre of the crystal, Fig. 2f, the injection is blocked and the wall is generated, Figs. 2g and 2h. In this way a single DW is written at the desired location along the transverse dimension. Notice that more than one DW can be written if larger angles in the writing beam are used.

CHARACTERIZATION OF THE DWs

In order to fully characterize the features of the different DWs that are being observed, it is necessary to measure the complex field. This is achieved by means of the interferometric technique already used in [6]: A CCD video camera records the interference pattern between the near field (i.e., the intracavity field at the crystal plane) and a homogeneous reference beam. From the interferometric pattern, like those of Fig. 2, a Fourier transform technique allows the reconstruction of both the amplitude and phase of the optical field, see [6] for full details. Some comments are in order regarding the way data must be extracted and processed.

An important feature that must be pointed out is that the spatial profile of the emitted field is not flat, as can be appreciated in Fig. 3. Of course one cannot expect a perfectly flat profile as the pumping fields are Gaussian, but the interesting point is that the more positive cavity detuning is the less flat and less extended the output profile is, i.e., there is a noticeable self-focusing effect [24, 25]. This is particularly relevant in the "free" transverse dimension (x direction in Fig. 3, which is the direction that is not limited by the intracavity diaphragms).

This fact is at the origin of one effect that has to be taken into account when characterizing the DW dynamics: The variation of the intensity profile along the x di-

mension is quite strong, stronger than for negative detuning, and no simple experimental arrangement can cope with this. We shall come back to this point in the following section when studying the dynamics of Bloch walls as x is the direction along which Bloch walls move.

Apart from these nonuniformities along the x direction, one has to take into account also the nonuniformities along the direction of the DW, i.e., the y direction, see Fig. 3. The finite extension of the pump as well as the already commented self-focusing effect make that the output intensity departs noticeably from a top hat profile. This fact affects the nature of the DW as it cannot be strictly uniform in the y direction thus making necessary to discard the borders of the illuminated region in order to characterize DWs properly.

Let us consider, for example, the interferogram corresponding to a static wall shown in Fig. 4a. For the reconstruction of the field amplitude and phase first we must choose between taking data for a particular value of y or making an average for different values of y . We choose the second option in order to smooth the effect of any local imperfection. Then we average the field obtained from the interferometric technique [6] and obtain the average field $\langle A(x) \rangle_y$. But before we must decide if we consider all data or we take into account only the central part (in the y direction): If only the central part of the interferogram is considered for reconstructing the field amplitude and phase, one obtains the profile of an Ising wall, Fig. 4b, with null intensity at the center and a sharp phase jump. Contrarily, if one does not discard the borders and takes all data into account, one obtains a profile that does not correspond so clearly to an Ising wall, as can be seen in Fig. 4c (the intensity does not reach zero and the phase jump is smoother). Of course this is nothing but the influence of a border effect that is due to the already commented nonuniformity of the fields along the y direction, and indicates the way in which data must be treated because the Ising character of the DW is clear from its dynamics: They are static.

In the case of moving walls the border effect is not so noticeable: Fig. 5a shows a typical interferogram of a moving wall and the corresponding averages of the reconstructed field (without borders in Fig. 5b and with them in Fig. 5c). In this case the wall moves from right to left and it is interesting to notice that the field amplitude on the left side of the Bloch wall is smaller than that of the right side. This occurs always: the intensity is larger on the back side of the wall with respect the direction of movement, a feature that is reproduced with the simple model used in [15] for reproducing a hysteretic NIBT.

Then the experimental procedure consists in injecting a single DW, recording the interferogram, extracting the information about intensity, phase gradient and spatial position of a single DW for different instants of time, and repeating this procedure for different values of the cavity detuning.

DYNAMICS OF DWS

In this section we deal with the dynamics of DWs in our particular non flat background profile. Fig. 6 shows the trajectories followed by both a static wall and a moving one that were created at the same spatial position (the centre of the nonlinear crystal). As commented below, the static walls shows some slow dynamics.

The static wall is an Ising wall, as its intensity and phase profiles for different instants of time, shown in Fig. 7, clearly show. One can observe that after an initial transient in which the intensity does not reach zero and the phase jumps are relatively smooth, the intensity and phase profiles progressively approach those of an Ising-type: After the transient, the change of phase through the interface is quite abrupt and the intensity at the center of the wall is very close to zero. It must also be noticed that the amplitude of the field on the right and on the left of the DW are similar. The initial movement can be easily attributed to the transient behaviour that occurs until the DW reaches its final profile. The remaining movement must be attributed to noise as the trajectory shows more a wandering behaviour than a systematic one. The above completely characterizes static DWs that are clearly identified as Ising DWs.

Let us now consider moving walls. In Fig. 8 we display their intensity and phase profiles, again for different time values. The behaviour is very different from that of the static wall of Fig. 7: The moving DW moves continuously to the left, its velocity changes with time, and the intensity and phase also change during the motion. We can conclude that it is a Bloch wall (smooth change of phase and nonzero intensity at the core of the wall). The fact that the velocity is not constant can be attributed to the fact that for the different positions the DW is placed on a different background as the intensity decreases towards the borders of the illuminated region, Fig. 3. In other words, the acceleration shown by the DW can be attributed to the existence of an intensity gradient in the field. It is also to be noted that the intensity in the left side of the DW is smaller than that in the right side, and also that this effect increases as the wall approaches the border of the illuminated region. We have checked that all these features are captured by a simple model for DW dynamics (a Ginzburg–Landau equation with broken phase symmetry, see [5]) when pump is spatially inhomogeneous.

Looking at how intensity and phase change during the accelerated motion, one can qualitatively conclude that the larger the wall velocity is, the larger (smaller) the intensity (the phase gradient) at the centre of the wall is. These facts make it difficult the determination of the DW velocity for a given set of parameters: Our procedure has consisted in taking an average velocity in those cases in which it is more or less constant, discarding al-

ways the velocities corresponding to the regions located close to the border of the illuminated region (where the acceleration is more obvious).

The measurements we have just commented correspond to a particular value of the cavity detuning. In order to see how a change in this parameter affects the moving DW, we show in Fig. 9 the intensity and phase profiles for three different values of the cavity detuning but corresponding to approximately the same position on the transverse direction, i.e., to the same intensity background. We observe again that for increasing detuning the velocity increases and, again, the more velocity the wall gets, the more intensity and less phase gradient it has.

To sum up, we can conclude that there is experimental evidence of the connection between the DW velocity and the characteristics of the optical field at the centre of the interface: The smoother the phase jump is and the larger the intensity at the wall core is, the faster the DW is.

CHIRALITY

In the previous section we have shown how the intensity and phase gradient of the DW change with detuning and background conditions. We pass now to a more quantitative study of the relation existing between the intensity at the core of the DW, I_0 , and the phase gradient, $\nabla\phi_0$.

In Fig. 10 we represent, in a log–log plot, $\nabla\phi_0$ versus I_0 for fixed parameters, the different points corresponding to different time instants (it is a parametric plot). It is clear that a linear fit is well suited, which leads to the relation

$$I_0^m \nabla\phi_0 = 10^{-n}, \quad (1)$$

where the typical values for the slope and crossing point are $m = -0.56$ and $n = 2.12$, respectively, and the coefficient of determination R–squared has a value of 0.9989. A similarly good correlation is also found for other detuning values, although m and n change slightly with detuning (m varies between -0.67 and -0.56 , and n varies between 2.32 and 2.12). It is obvious that these fits do not allow saying that m and n are constant, but we think that their change with detuning could be attributed to a corresponding change with detuning in the shape and intensity of the background (due to the already commented self–focusing effect). In any case, this result invites to try to describe the dynamics in terms of only one magnitude of the field at the interface, either the phase gradient or the intensity or a combination of both.

As already commented, Bloch walls are chiral structures as the complex field can rotate in the complex plane when passing from one side to the other of the DW with two different directions [5]. This has an important physical consequence, as Bloch walls with different chiralities

move in opposite directions [5]. In [8] a chirality parameter defined as

$$\chi = I_0 \nabla\phi_0, \quad (2)$$

was used for characterizing the DW dynamics (other definitions of the chirality can be proposed). For Ising walls the chirality parameter is zero and the wall remains static, whilst for Bloch walls the chirality is non zero and the wall moves with a velocity proportional to the value of χ .

From our experimental results we can now justify the use of (2) as a quantity that characterizes the DW dynamics. In Fig. 11 a linear fit between the velocity and the chirality parameter of a DW, as it evolves with time, is shown for a particular value of the detuning. It is worth stressing that the measurement of the velocities is not so reliable as the measurement of intensity and phase, for the reasons commented above, and for this reason the linear fit is not so good as that of Fig. 10. We have also tried using other quantities as the chirality, the results in Fig. 11 being the best (e.g., if one uses the intensity or the inverse of the phase gradient as chirality parameters, the correlations one obtains are 0.9540 and 0.9813, respectively, which are considerably smaller than the 0.9967 obtained in Fig. 11).

THE ISING–BLOCH TRANSITION

There remains to explain how the transition from Ising walls to Bloch walls (the nonequilibrium Ising–Bloch transition, NIBT) occurs as cavity detuning is increased. In fact this was the subject of Ref. [7]. We reproduce here a brief explanation of this for the sake of completeness.

In Fig. 12 a typical plot of the DW velocity as a function of cavity detuning is shown. The rare aspect of this NIBT is that it exhibits hysteresis: We start with a static wall at resonance and increase detuning until the DW starts moving, signaling an Ising–Bloch transition (this is marked as IBT in Fig. 12). For larger detuning values, DWs always move. Then, from a large positive detuning, we inject a DW and check whether it moves or not, and repeat this operation for decreasing detuning values until we obtain a static (Ising) wall (this is marked as BIT in Fig. 12). The interesting thing is that the two NIBTs occur at different detuning values. In other words, there is a finite detuning range (between BIT and IBT) where, for fixed detuning, we obtain either Ising or Bloch walls in subsequent injections.

Notice that the bistability range and the velocity values in Fig. 12 are smaller, roughly by a factor of 50%, than those reported in [7]. The reason is that the two cases correspond to two different experiments with different gains what obviously affects the DW dynamics quantitatively.

Let us finally comment that a simple model that predicts a hysteretic NIBT like the one we have just commented can be found in [15]. In this model one finds that the origin of the hysteresis lies on the existence of bistability in the homogeneous solutions of the system, a bistability that we have also found in the experiment. We refer the interested reader to [7, 15] for further details.

CONCLUSIONS

In conclusion, we have reported a detailed experimental characterization of domain walls dynamics in a nonlinear optical cavity, namely a photorefractive oscillator working in a degenerate four-wave mixing configuration. An injection technique to remove any spontaneous initial structure and to write a single DW at any desired location has been shown. The dynamics of the DWs has been characterized in terms of the intensity and phase gradient of the optical field. We have also shown the relation existing between these two quantities that leads naturally to the identification of the chirality parameter. Finally, the hysteretic nonequilibrium Ising–Bloch transition, which turns out to be hysteretic in our case, has been shown.

Acknowledgements

This work has been financially supported by the Spanish Ministerio de Ciencia y Tecnología and European Union FEDER (Projects BFM2002-04369-C04-01, FIS2004-06947-C02-01 and FIS2005-07931-C03-01), and by the Agència Valenciana de Ciència i Tecnologia of the Valencian Government (Project GRUPOS03/117). V.B.T. was financially supported by the Spanish Ministerio de Educación, Cultura y Deporte (grant SAB2002-0240).

- [8] G.J. de Valcárcel, I. Pérez–Arjona, and E. Roldán, *Phys. Rev. Lett.* **89**, 164101 (2002).
- [9] T. Frisch, S. Rica, P. Couillet, and J. M. Gilli, *Phys. Rev. Lett.* **72**, 1471 (1994).
- [10] T. Kawagishi, T. Mizuguchi, and M. Sano, *Phys. Rev. Lett.* **75**, 3768 (1995).
- [11] I. Pérez–Arjona, F. Silva, G. J. de Valcárcel, E. Roldán and V. J. Sánchez–Morcillo, *J. Opt. B: Quantum Semiclass. Opt.* **6**, S361 (2004).
- [12] G. Izús, M. San Miguel and M. Santagiustina, *Opt. Lett.* **25**, 1454 (2000).
- [13] D. Michaelis, U. Peschel, F. Lederer, D. V. Skryabin, and W. J. Firth, *Phys. Rev. E* **66**, 066602 (2001).
- [14] V.J. Sánchez–Morcillo, V. Espinosa, I. Pérez–Arjona, F. Silva, G.J. de Valcárcel and E. Roldán, *Phys. Rev. E* **71**, 066209 (2005)
- [15] V.B. Taranenko, A. Esteban–Martín, G.J. de Valcárcel, and E. Roldán, e–print nlin.PS/0510018.
- [16] J. A. Arnaud, *Appl. Opt.* **8**, 189 (1969).
- [17] V. B. Taranenko, K. Staliunas, and C. O. Weiss, *Phys. Rev. Lett.* **81**, 2236 (1998).
- [18] A. Esteban–Martín, J. García, E. Roldán, V.B. Taranenko, G.J. de Valcárcel, and C.O. Weiss, *Phys. Rev. A* **69**, 033816 (2004).
- [19] P. Yeh, *Introduction to Photorefractive Nonlinear Optics* (Wiley & Sons, New York, 1993)
- [20] M. Vaupel and C. O. Weiss, *Phys. Rev. A* **51**, 4078 (1995).
- [21] K. Staliunas, G. Sleky, and C. O. Weiss, *Phys. Rev. Lett.* **79**, 2658 (1997).
- [22] A. V. Mamaev and M. Saffman, *Opt. Commun.* **128**, 281 (1996).
- [23] A. Esteban–Martín, V.B. Taranenko, E. Roldán, and G.J. de Valcárcel, *Opt. Express* **13**, 3631 (2005)
- [24] We note that for negative cavity detuning (where a stripe pattern is observed, see [18]) a wide output beam is obtained in the x direction. As detuning is made positive and increased the output beam becomes increasingly narrower in the “free” transverse dimension. This observation is compatible with the observations in [25].
- [25] M. Vaupel, O. Mandel, and N.R. Heckenberg; *J. Opt. B: Quantum Semiclass. Opt.* **1**, 96 (1999)
- [26] S. Trillo, M. Haelterman, and A. Sheppard, *Opt. Lett.* **22**, 970 (1997).

-
- [1] P. Manneville, *Dissipative Structures and Weak Turbulence* (Academic Press, 1990).
 - [2] M. C. Cross and P. C. Hohenberg, *Rev. Mod. Phys.* **65**, 851 (1993).
 - [3] D. Walgraef, *Spatio-Temporal Pattern Formation* (Springer, Berlin, 1996).
 - [4] K. Staliunas and V. J. Sánchez–Morcillo, *Transverse Patterns in Nonlinear Optical Resonators* (Springer, Berlin, 2002).
 - [5] P. Couillet, J.Lega, B. Houchmanzadeh, and J. Lajzerowicz, *Phys. Rev. Lett.* **65**, 1352 (1990).
 - [6] Ye. Larionova, U. Peschel, A. Esteban–Martín, J. García Monreal, and C.O. Weiss, *Phys. Rev. A* **69**, 033803 (2004).
 - [7] A. Esteban–Martín, V.B. Taranenko, J. García, G.J. de Valcárcel, and E. Roldán, *Phys. Rev. Lett.* **94**, 223903 (2005).

FIGURE CAPTIONS

Fig. 1.- Scheme of the experimental setup. M: cavity mirrors; l : effective cavity length; D: diaphragm located in the Fourier plane (FP) that makes the system quasi-1D; PM: piezo-mirror for control of the cavity detuning; CCD: cameras to take pictures from near field; and L: lenses.

Fig. 2.- Experimental interferometric snapshots of the domain wall injection process. a) Initial homogeneous field, b) injection is applied, c)-e) a domain wall appears and moves, f) the injected wall is located at the centre of the crystal, g) the injection beam is blocked, and h) the domain wall is finally written. Time runs from top to bottom in steps of 5 s. The transverse dimension is 1.6 mm.

Fig. 3.- Experimental snapshot of a 3D view of the emitted field containing a domain wall.

Fig. 4.- Experimental interferometric snapshot of a static domain wall (a), reconstructed amplitude and phase neglecting the boundaries (b), and reconstructed amplitude and phase taking into account the boundaries (c). The cavity detuning is zero.

Fig. 5.- Experimental interferometric snapshot of a static domain wall (a), reconstructed amplitude and phase neglecting the boundaries (b), and reconstructed amplitude and phase taking into account the boundaries (c). The cavity detuning is 12% of the free spectral range (FSR). The FSR of the cavity is 120Mhz.

Fig. 6.- Plot of the trajectories of a static (full line) and a moving (dashed line) domain wall that were gen-

erated at the same spatial position. The detuning for the static and moving wall are zero and 20% of the free spectral range, respectively.

Fig. 7.- Reconstructed amplitudes (top) and phases (bottom) corresponding to a static domain wall at different instants (the time interval between different profiles is 5s). The different location of the phase gradients (bottom) is artificial and has been introduced for the sake of clarity (this applies also to Fig. 8).

Fig. 8.- As Fig. 7 but for a moving domain wall. The time interval between different profiles is 2s.

Fig. 9.- Reconstructed amplitudes and phases of domain walls located at the same spatial position but obtained for different detunings. Detuning increases from left to right (in percentage of the free-spectral range): a) 0 % , b) 10 % and c) 20 %. Velocity increases as detuning does: a) $0 \mu\text{m.s}^{-1}$, b) $7 \mu\text{m.s}^{-1}$, and c) $12 \mu\text{m.s}^{-1}$.

Fig. 10.- Logarithm of the intensity at the core of the DW, I_0 , versus the logarithm of the phase gradient, $\nabla\phi_0$, for different instants and fixed detuning (20% of the free-spectral range). Squares correspond to experimental data and the straight line correspond to the fit.

Fig. 11.- Relation between the velocity of a moving domain wall and the chirality parameter measured during its motion in a non flat background field. Squares correspond to the experimental data and straight lines correspond to the linear fit.

Fig. 12.- Velocity of the DWs as a function of cavity detuning. BIT and IBT mark the two nonequilibrium Ising-Bloch transitions. See text for more details.

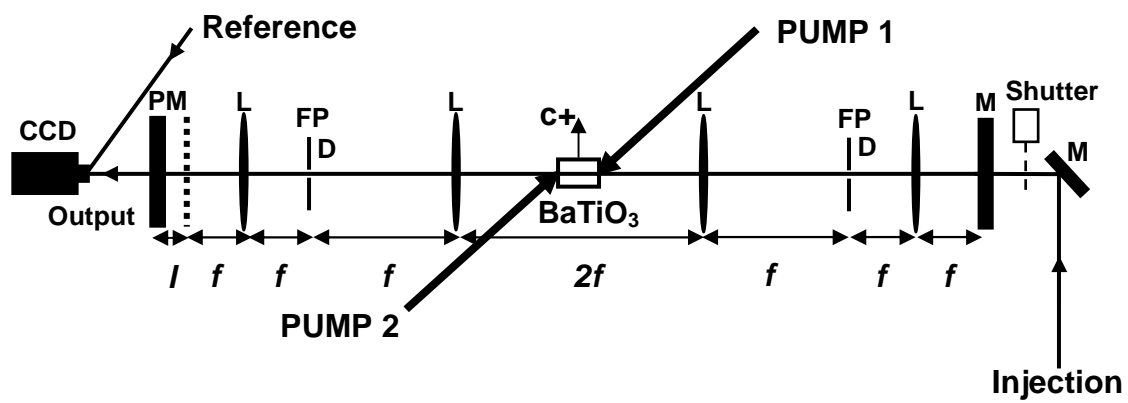


Figure 1

A. Esteban-Martín et. al, *Experimental characterization of domain walls...*

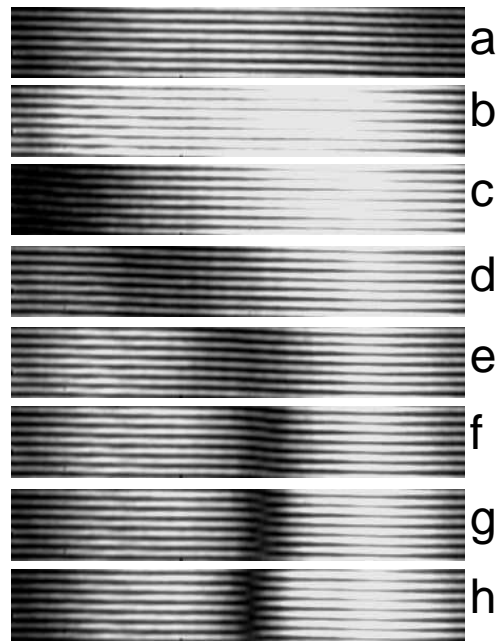


Figure 2

A. Esteban-Martín et. al, *Experimental characterization of domain walls...*

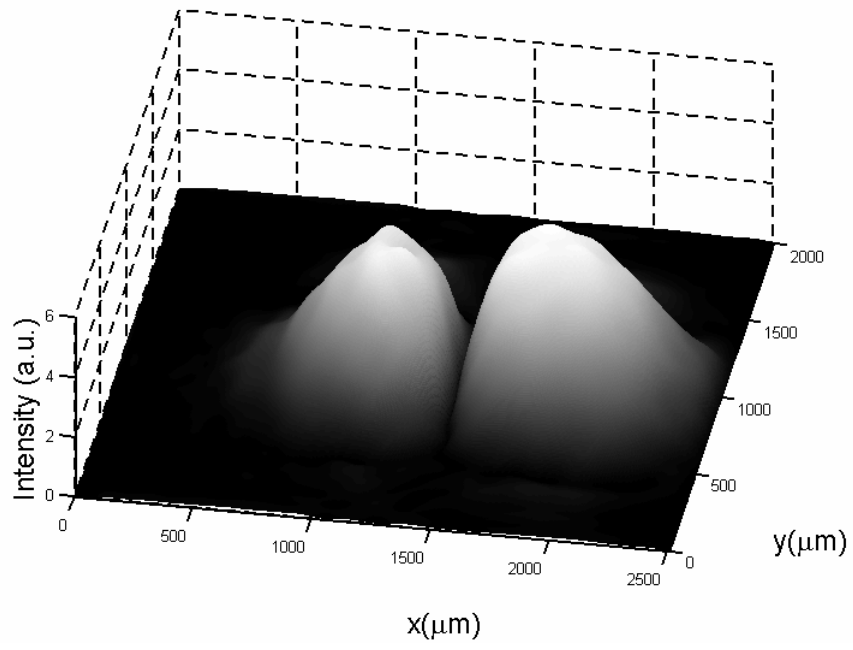


Figure 3

A. Esteban-Martín et. al, *Experimental characterization of domain walls...*

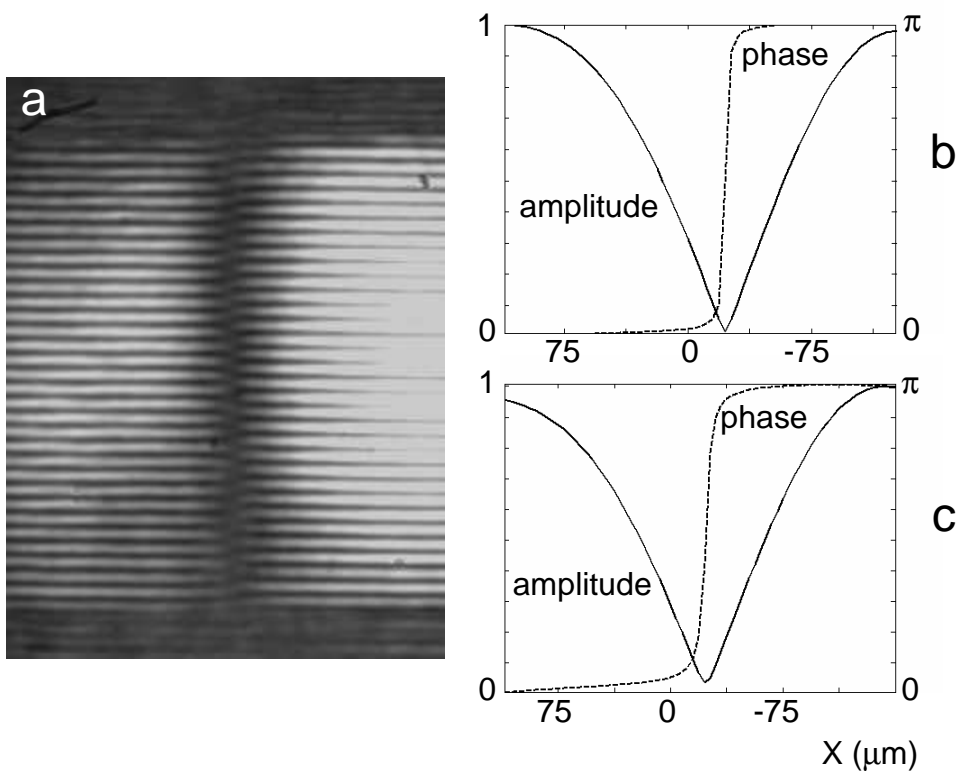


Figure 4

A. Esteban-Martín et. al, *Experimental characterization of domain walls...*

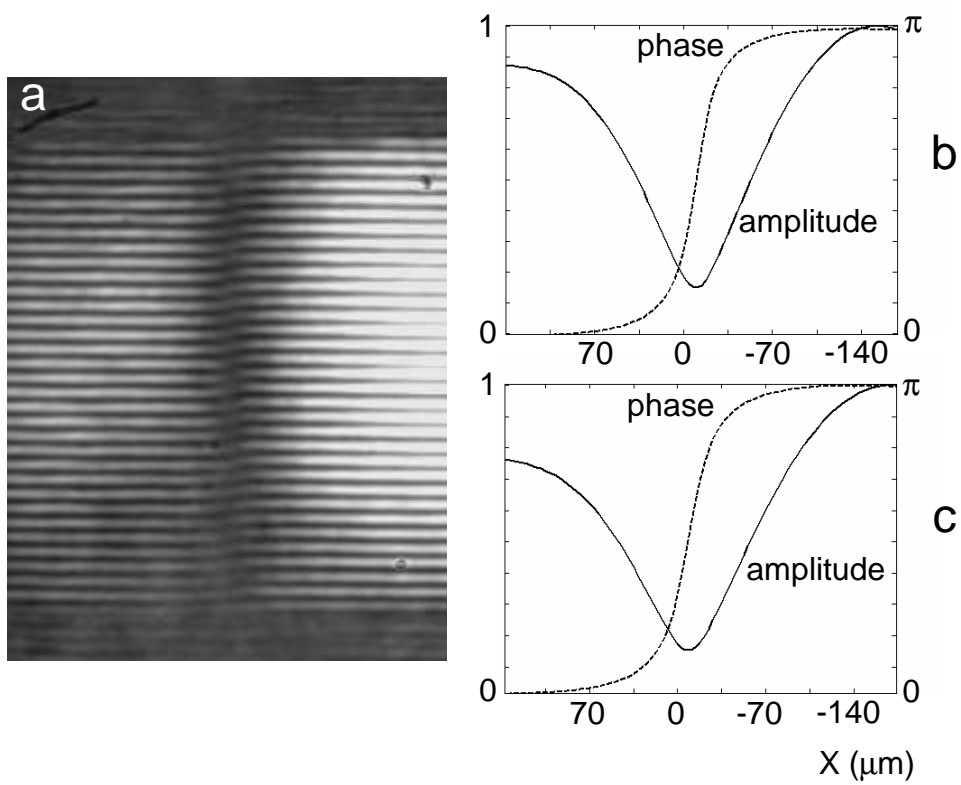


Figure 5

A. Esteban-Martín et. al, *Experimental characterization of domain walls...*

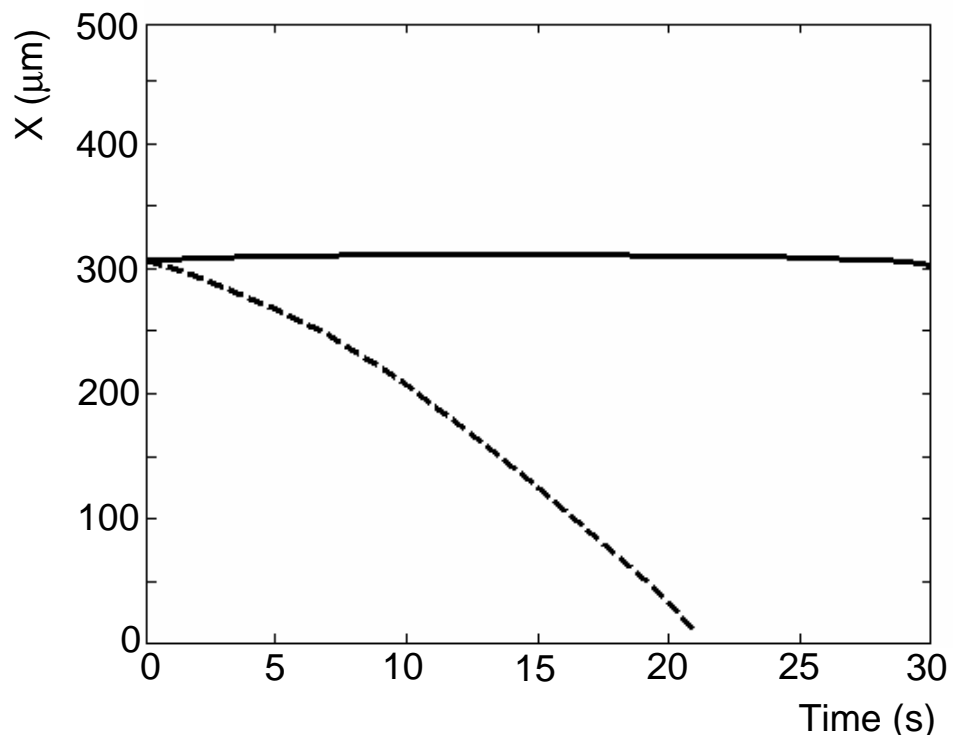


Figure 6

A. Esteban-Martín et. al, *Experimental characterization of domain walls...*

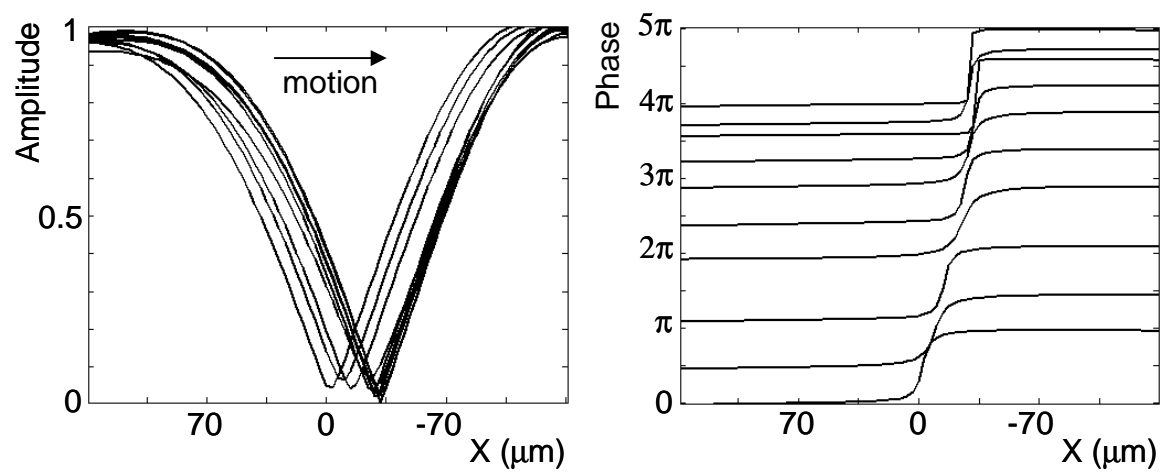


Figure 7

A. Esteban-Martín et. al, *Experimental characterization of domain walls...*

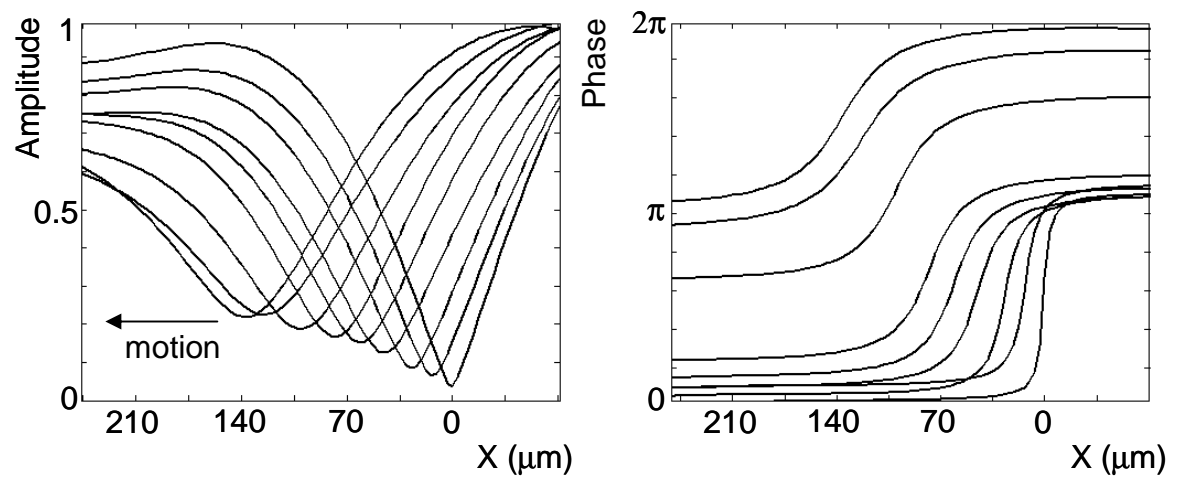


Figure 8

A. Esteban-Martín et. al, *Experimental characterization of domain walls...*

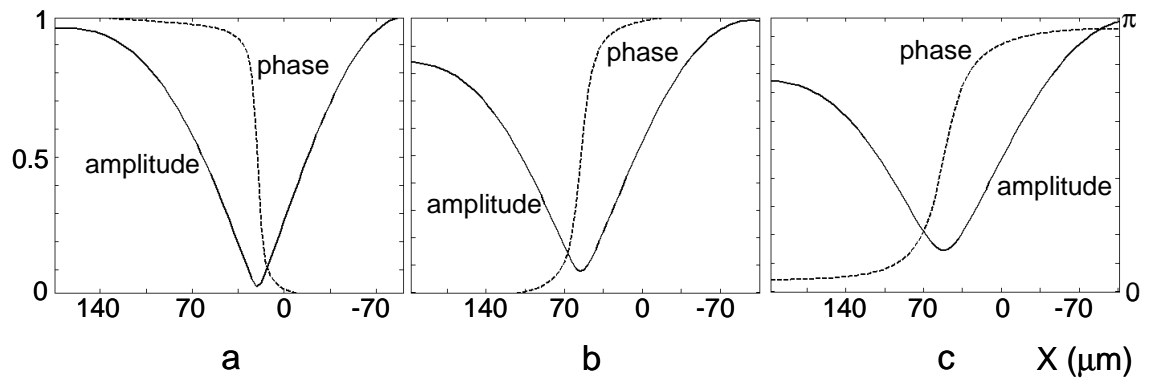


Figure 9

A. Esteban-Martín et. al, *Experimental characterization of domain walls...*

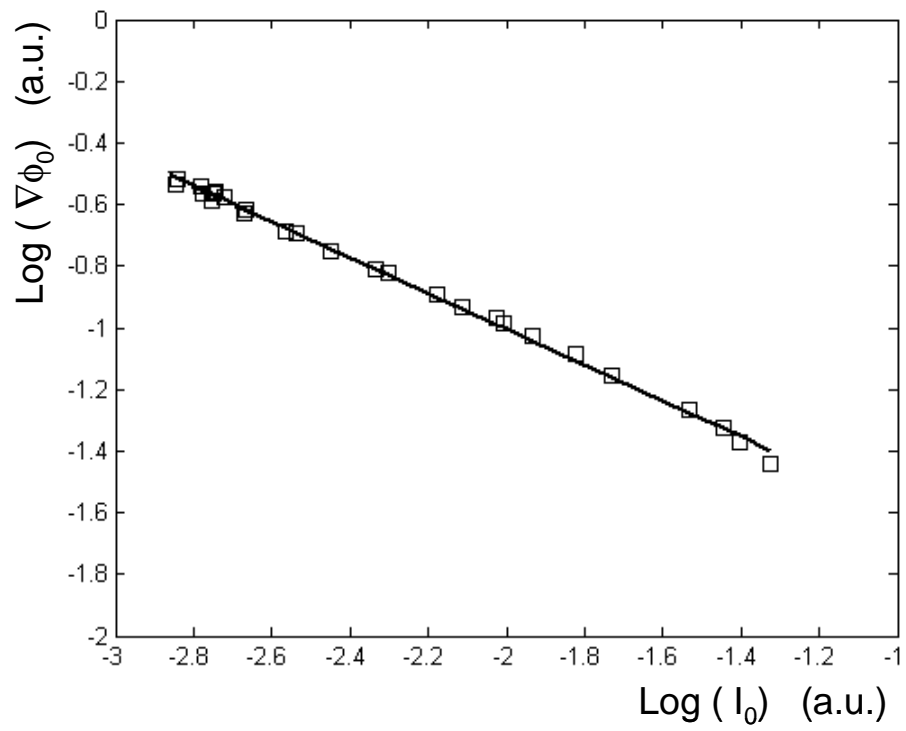


Figure 10

A. Esteban-Martín et. al, *Experimental characterization of domain walls...*

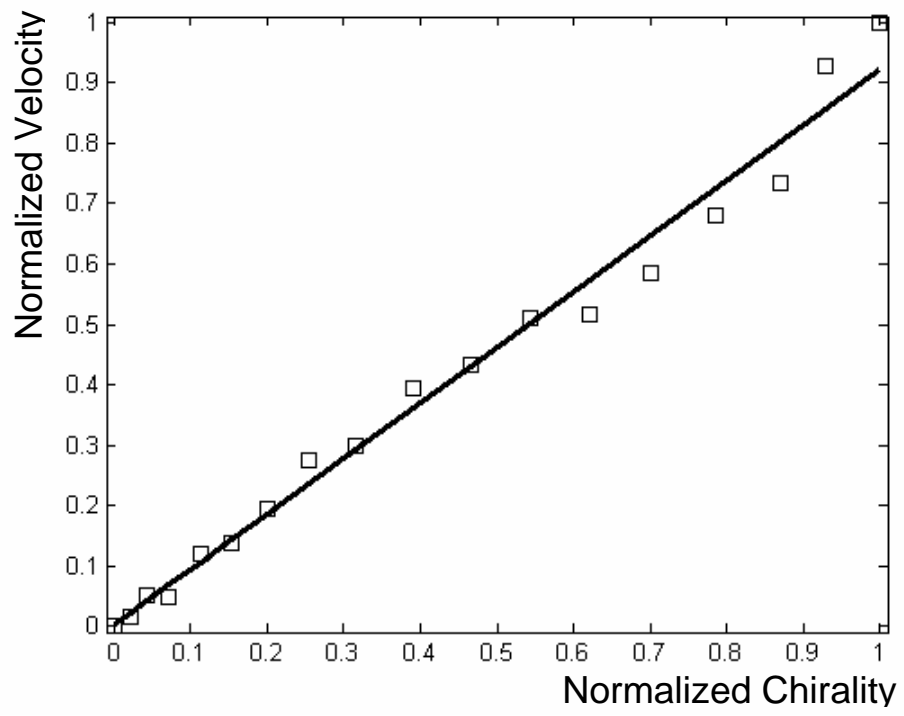


Figure 11

A. Esteban-Martín et. al, *Experimental characterization of domain walls...*

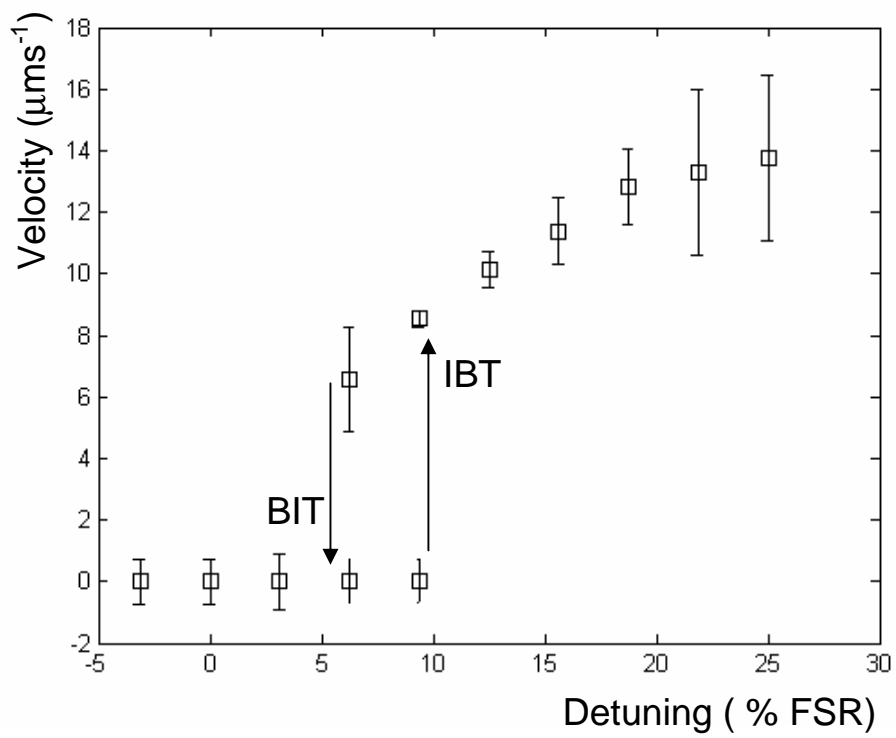


Figure 12

A. Esteban-Martín et. al, *Experimental characterization of domain walls...*